

# We are IntechOpen, the world's leading publisher of Open Access books Built by scientists, for scientists

6,900

Open access books available

186,000

International authors and editors

200M

Downloads

Our authors are among the

154

Countries delivered to

TOP 1%

most cited scientists

12.2%

Contributors from top 500 universities



WEB OF SCIENCE™

Selection of our books indexed in the Book Citation Index  
in Web of Science™ Core Collection (BKCI)

Interested in publishing with us?  
Contact [book.department@intechopen.com](mailto:book.department@intechopen.com)

Numbers displayed above are based on latest data collected.  
For more information visit [www.intechopen.com](http://www.intechopen.com)



# Preparation of Functionalized Hydroxyapatite with Biopolymers as Efficient Adsorbents of Methylene Blue

*Hassen Agougui, Youssef Guesmi and Mahjoub Jabli*

## Abstract

In this study, we reported the synthesis of hydroxyapatite modified with biopolymers as  $\lambda$ -carrageenan and sodium alginate, which could be used as effective adsorbents of cationic dyes. Evidence of chemical modification was proved through chemical analysis, Fourier Transform Infrared spectroscopy, powder X-ray diffraction, scanning electron microscopy, and specific surface area. The adsorption process was studied using methylene blue as representative cationic dye. The adsorbed quantity reached, at equilibrium, 142.85 mg/g and 98.23 mg/g using hydroxyapatite-sodium alginate and hydroxyapatite-( $\lambda$ -carrageenan), respectively. However, it does not exceed 58.8 mg/g in the case of the unmodified hydroxyapatite. The adsorption of methylene blue using hybrid materials complied well with the pseudo-second-order suggesting a chemisorption. Freundlich and Langmuir isotherm described well the adsorption mechanism of the hydroxyapatite-( $\lambda$ -carrageenan) and hydroxyapatite-sodium alginate, respectively. The high capacities of MB removal obtained in this study suggest the potential use of these materials in the treatment from wastewaters.

**Keywords:** hydroxyapatite, biopolymer alginate, dye, kinetic

## 1. Introduction

Contaminated waters can be successfully treated using inexpensive adsorbents. In this sense, many biopolymers were proposed including cellulose [1–3], chitosan [4, 5], chitin [6, 7], etc. Hybrid materials have attracted a particular attention. The interaction between calcium hydroxyapatite and biopolymers has been the subject of many studies such as carboxymethyl cellulose [8], polygalacturonic acid [9], collagen [10], Agar-Agar [11], polycaprolactone [12], banana peel [13], chitosan [14], and gelatin [15]. Currently, the application of hydroxyapatite modified by biopolymers for immobilization of various pollutants has been considered as a promising pollution control technology [16–20]. For example, Huijuan and colleagues [21] have, recently, reported interesting results about the preparation of hydroxyapatite-Chitosan composite and its efficiency for the removal of Congo red dye from aqueous solution.

The results indicate that the kinetic and isotherm studies showed that pseudo-second-order model and Langmuir model could well describe the

adsorption behavior, while thermodynamic investigation of Congo red adsorption by hydroxyapatite-Chitosan composite confirmed a spontaneous adsorption. It has been demonstrated that this composite is an effective and low-cost adsorbent for the dye-polluted water purification [21].

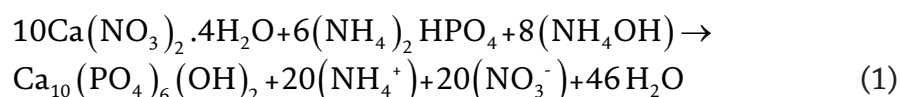
In the same framework, the present work describes the synthesis of hybrid compounds CaHAp-Alginate and CaHAp-(Carrageenan) as an adsorbent using a facile method by varying the content of the bio-polymer. Evidence of interaction between hydroxyapatite and Alg or ( $\lambda$ -Carr) was confirmed using various techniques including FT-IR, SSA, DRX and SEM. The factors that influence the dye uptake by the prepared adsorbents were also investigated and discussed.

## 2. Experimental

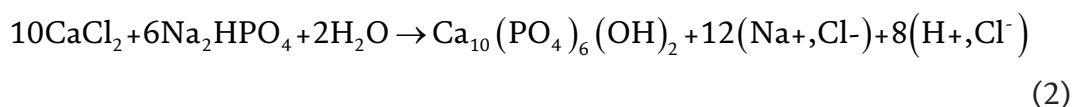
### 2.1 Synthesis of hydroxyapatite (CaHAp1 and CaHAp2)

Hydroxyapatite was synthesized via co-precipitation method [22, 23]. As starting reagents, analytical grade  $\text{CaCl}_2$ ,  $\text{Na}_2\text{HPO}_4$ ,  $\text{Ca}(\text{NO}_3)_2 \cdot 4\text{H}_2\text{O}$ ,  $(\text{NH}_4)_2\text{HPO}_4$  and  $\text{NH}_4\text{OH}$  were used. The chemicals equations that describes the reactions is given as follow:

#### CaHAp1



#### CaHAp2



An aqueous solution of 250 mL of  $\text{Ca}(\text{NO}_3)_2 \cdot 4\text{H}_2\text{O}$  or  $\text{CaCl}_2$  (0.2 M) was added drop-wise to 150 mL of  $(\text{NH}_4)_2\text{HPO}_4$  or  $\text{Na}_2\text{HPO}_4$  (0.2 M) solution under  $\text{N}_2$  bubbling with a stoichiometric ratio of  $\text{Ca}/\text{P} = 1.67$ .

The pH was adjusted to 10 by adding  $\text{NH}_4\text{OH}$  solution gradually. After the complete addition, the suspension was matured for 72 h at room temperature under magnetic stirring, the resultant precipitate was filtered, washed with distilled water, and dried overnight at  $80^\circ\text{C}$ .

### 2.2 Synthesis of hydroxyapatite modified by sodium alginate CaHAp1-Alg

A similar procedure of CaHAp1 was adopted to synthesize the modified hydroxyapatite by sodium alginate CaHAp1-(Alg), except for the fact that the  $(\text{NH}_4)_2\text{HPO}_4$  was prepared with x mass of sodium alginate (5%, 10% or 20% of the total mass of  $\text{Ca}(\text{NO}_3)_2 \cdot 4\text{H}_2\text{O}$  in the starting solution).

### 2.3 Synthesis of hydroxyapatite modified by sodium alginate CaHAp1-( $\lambda$ -Carr)

CaHAp2-(Carr) was synthesized, following a similar procedure of CaHAp2, except for the calcium containing solutions that were prepared by mixing 0.05 moles of  $\text{CaCl}_2$  with x mol ( $x = 0.0025, 0.005$  and  $0.01$ ) of ( $\lambda$  Carr).

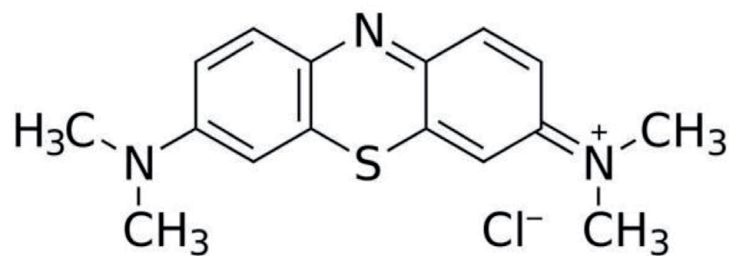


**Figure 1.**  
Structure of methylene blue.

In the text, Hydroxyapatite modified with ( $\lambda$ -Carr) is abbreviated as (CaHAp-(Carr) n), where n represents the mass ratio  $\frac{m(\text{Carr})}{m(\text{calcium})} \times 100$ .

## 2.4 Adsorption experiments

MB (its structure is given in **Figure 1**) solution was prepared by dissolving the calculated powder dye in distilled water with different required concentrations. NaOH and acetic acid solutions were used for adjusting the pH of the dye solution. For the adsorption experiments, MB solution was mixed with modified hydroxyapatite. MB concentrations were measured before and after experiments using a double beam UV-vis spectrophotometer (UV-1601 Shimadzu, Japan) at 664 nm. The adsorbed amount of dye onto modified hydroxyapatite (q mg/g) was calculated using the following equation [24]:

$$q_e = (C_o - C_e) \times \frac{V}{m} \quad (3)$$

Where  $C_o$  and  $C_e$  are the initial and equilibrium dye concentration (mg/L),  $V$  is the solution volume (mL) and  $m$  is the weight of used modified hydroxyapatite sample (g) for the adsorption.

## 3. Characterization techniques

The FT-IR spectra were recorded on a Perkin Elmer model 597 using KBr pellet method in the  $4000-400 \text{ cm}^{-1}$  region. X-ray powder diffractograms were obtained at room temperature on a PANalytical X'Pert PRO MPD equipped with copper anticathode tube. The morphological observation of the synthesized samples was undertaken using a JEOL JSM-5400 scanning electron microscope. Specific surface area (SSA) measurements were performed by BET-method (adsorptive gas  $\text{N}_2$ , carrier gas He, heating temperature  $100^\circ\text{C}$ ) using an Quantachrome Instruments, model: ASIM. LP2. The pH of the zero point charge ( $\text{pH}_{\text{ZPC}}$ ) was determined by putting 0.15 g of adsorbent in a closed Erlenmeyer flask containing 50 mL of NaCl solutions (0.1 M). The initial pH of these solutions was adjusted by either adding NaOH (0.1 M) or HCl (0.1 M) and were then agitated for 48 h at 150 rpm at room temperature to reach equilibrium. The final pH of supernatant was, further, measured and the  $\Delta\text{pH} = \text{pH}(\text{final}) - \text{pH}(\text{initial})$  was plotted against the initial pH. The pH at which  $\Delta\text{pH}$  was zero was taken as a  $\text{pH}_{\text{ZPC}}$ .

## 4. Results and discussion

### 4.1 Characterization of adsorbents

#### 4.1.1 X-ray diffraction

X-ray diffractograms of hydroxyapatite-Alg and hydroxyapatite-( $\lambda$ -Carr) are presented in **Figures 2** and **3**. For all compounds, the hydroxyapatite phase is conserved according to 00-024-0033 reference from the ICDD-PDF2 2003 database. However, in the case of CaHAp1-(Alg)20% new peaks appear at  $2\theta = 26.60^\circ$  and  $30.14^\circ$ . These peaks are characteristic of monetite phase ( $\text{CaHPO}_4$ ) according to 01-077-0128 reference from the ICDD-PDF2003 database. The increase of the amount of biopolymer induced the broadening of peaks, which proves their incorporation on the apatitic surface.

#### 4.1.2 FT-IR spectroscopy

**Figures 4** and **5** shows the FT-IR spectra of CaHAp, CaHAp-Alg and CaHAp-(Carr). In all IR spectra, the vibration bands of  $\text{PO}_4^{3-}$  groups of the apatite structure are observed at ( $\nu_s$ )  $965\text{ cm}^{-1}$ , ( $\delta_s$ )  $482\text{ cm}^{-1}$ , ( $\nu_{as}$ )  $1041\text{--}1094\text{ cm}^{-1}$  and ( $\delta_{as}$ )  $567\text{--}605\text{ cm}^{-1}$  [25]. Moreover, for characteristic bands of hydroxyl ions were observed towards ( $\nu_s$ )  $3572\text{ cm}^{-1}$  and ( $\nu_L$ )  $634\text{ cm}^{-1}$  [26].

The two broad bands located at  $1403\text{--}1462$  and  $1640\text{ cm}^{-1}$  were assigned, respectively, to the carbonate ions and water adsorbed on the surface. Besides, the band located at  $877\text{ cm}^{-1}$  was assigned to the ( $\text{HPO}_4^{2-}$ ) group [27].

After grafting, the intensity of the hydroxyls bands ( $\nu_s$  and  $\nu_L$ ) decrease progressively with increasing Alg or ( $\lambda$ -Carr) amount. This can be explained by the low degree of crystallinity [28].

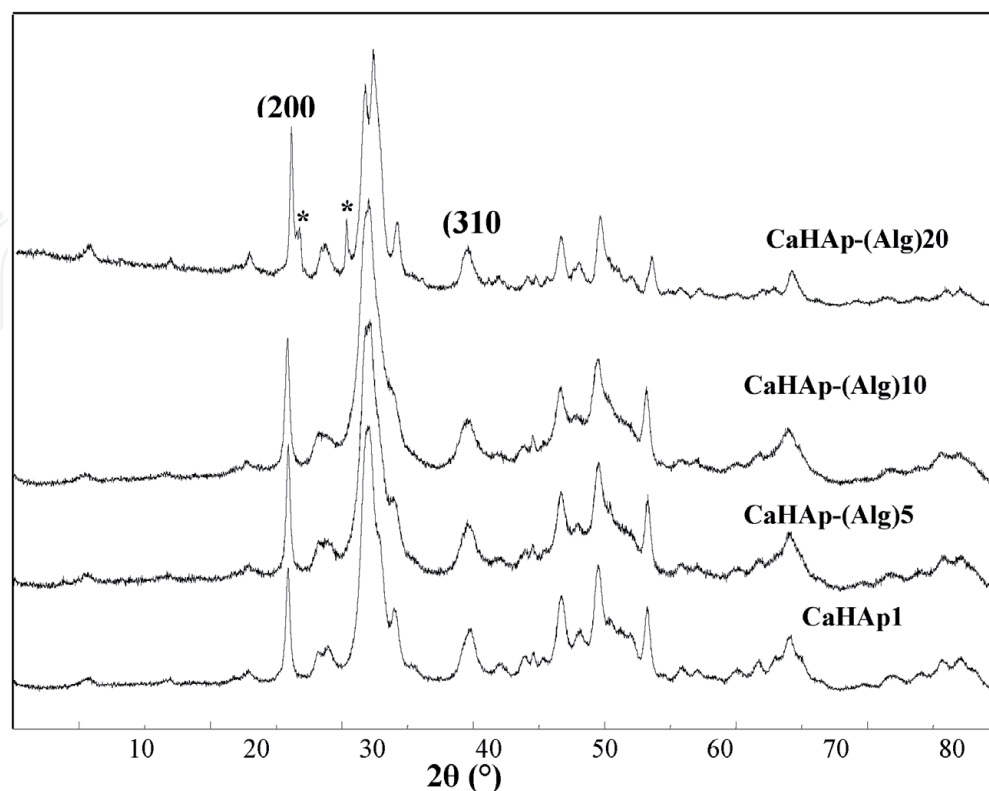


**Figure 2.**  
Powder x-ray diffraction patterns of modified hydroxyapatites by sodium alginate.

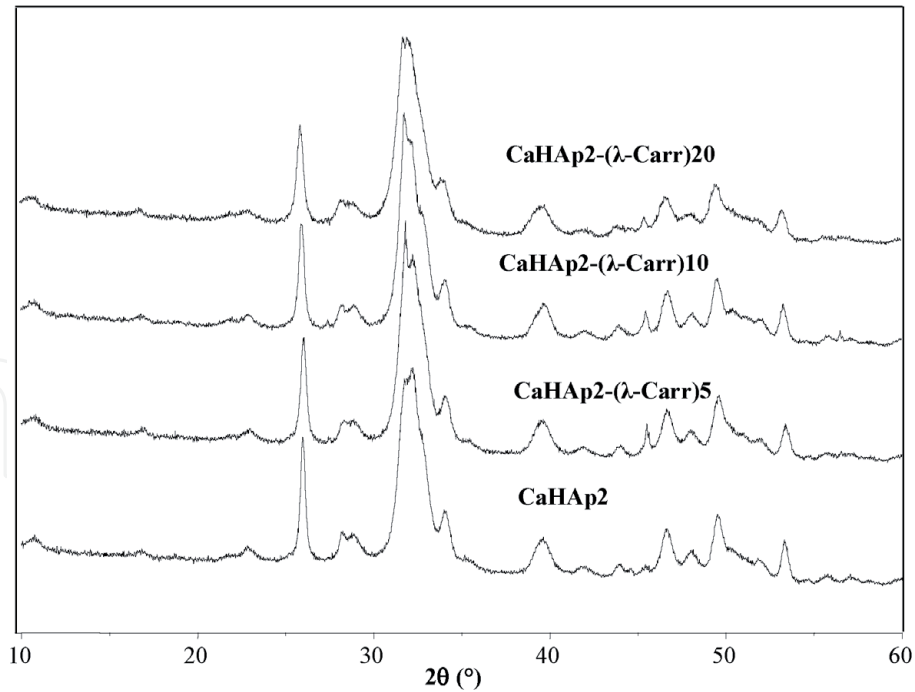


**Figure 3.**  
 Powder x-ray diffraction patterns of modified hydroxyapatites by lambda carrageenan.

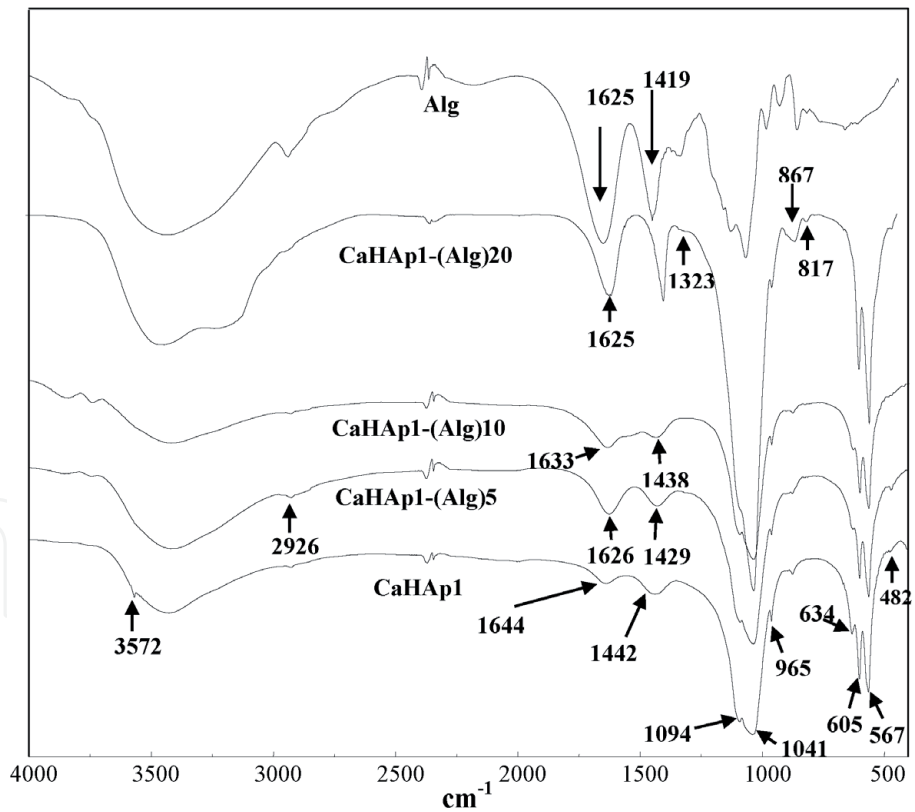


**Figure 4.**  
 FTIR spectra of modified hydroxyapatites by sodium alginate.

The presence of biopolymers (Alg or carr) on the apatitic surface is confirmed by the appears of new vibrations bands at 1231  $\text{cm}^{-1}$  and (1626, 1323 and 1428  $\text{cm}^{-1}$ ) which are assigned respectively, to S-O groups of ( $\lambda$ -Carr) and  $\text{COO}^-$  groups of (Alg) [29, 30].

On the other hand, the conservation in the band intensity of P-OH group at 870  $\text{cm}^{-1}$  indicates that fixing process of ( $\lambda$ -Carr) or Alg is done only by the interaction



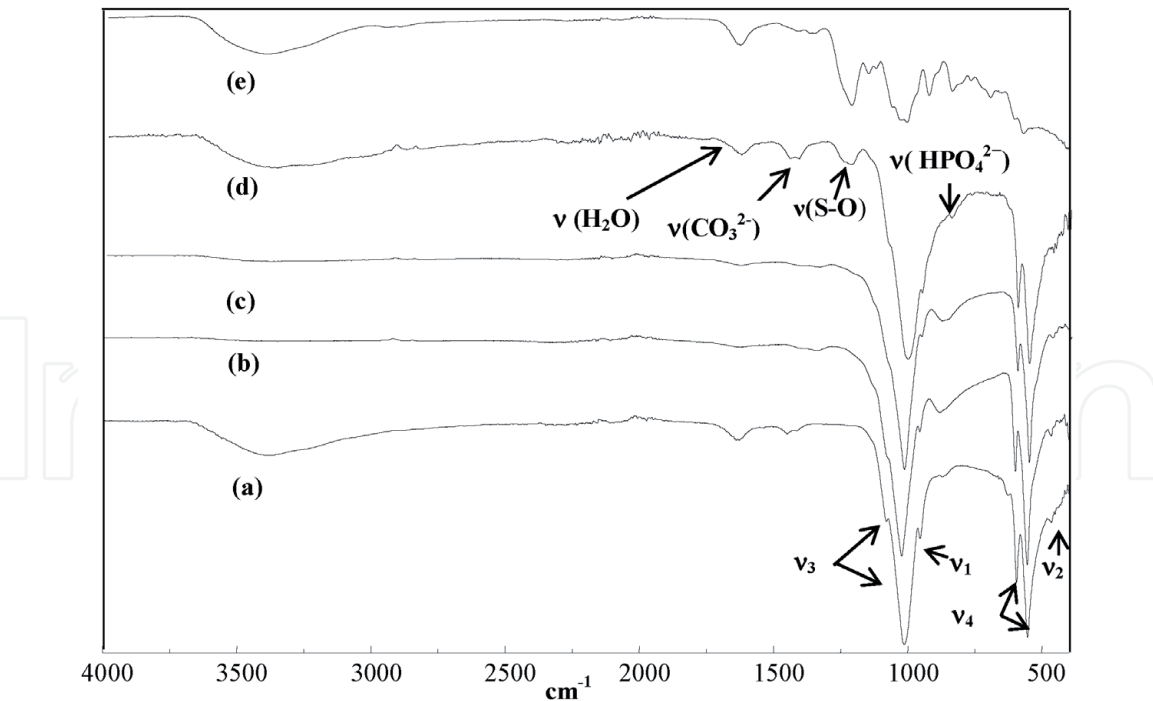


**Figure 5.**  
*FTIR spectra of modified hydroxyapatites by lambda carrageenan.*

between  $\equiv\text{Ca-OH}$  groups of apatitic surface and functional groups of each biopolymer.

The possible modes of interaction of (Alg) or ( $\lambda$ -Carr) with the CaHAp1 or CaHAp2 surface have been gathered in **Figures 6** and **7**.

4.1.3 Scanning electron microscope (SEM)

**Figure 8** shows the morphological variations of CaHAp1 or CaHAp1 before and after reaction with Alg or ( $\lambda$ -Carr). The CaHAp1 or caHap2 is composed of irregular particles with a strong tendency to aggregate (**Figure 8a, b**), whereas the modified hydroxyapatites showed that their shapes become relatively agglomerates

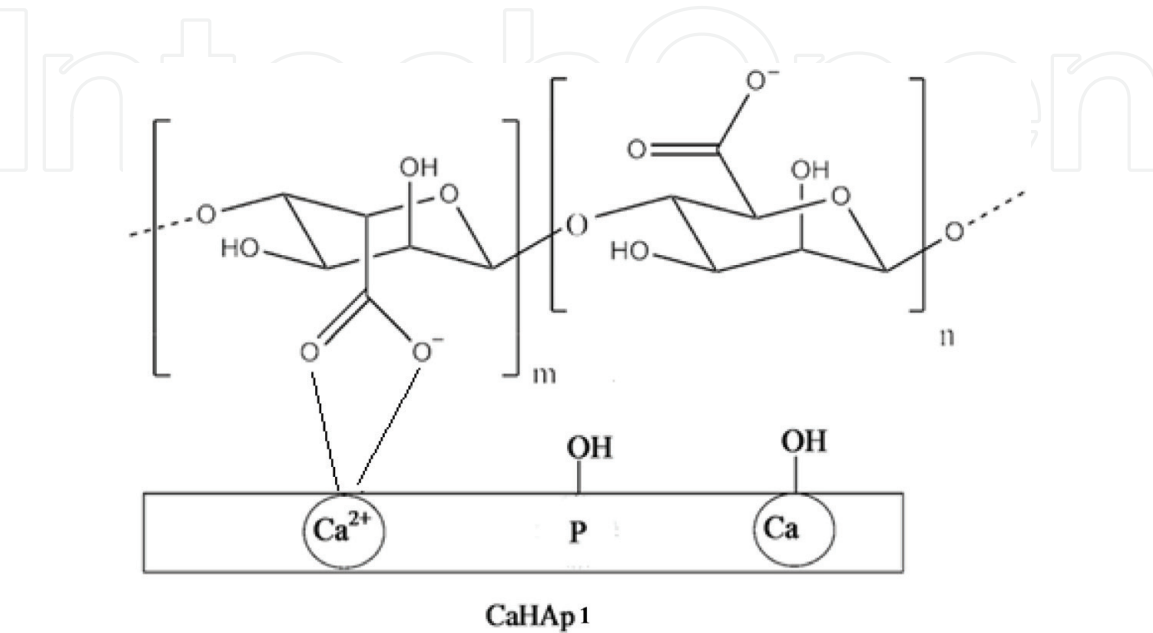


**Figure 6.**  
*Proposed mechanism of the interaction between Alg and CaHAp1 surface.*

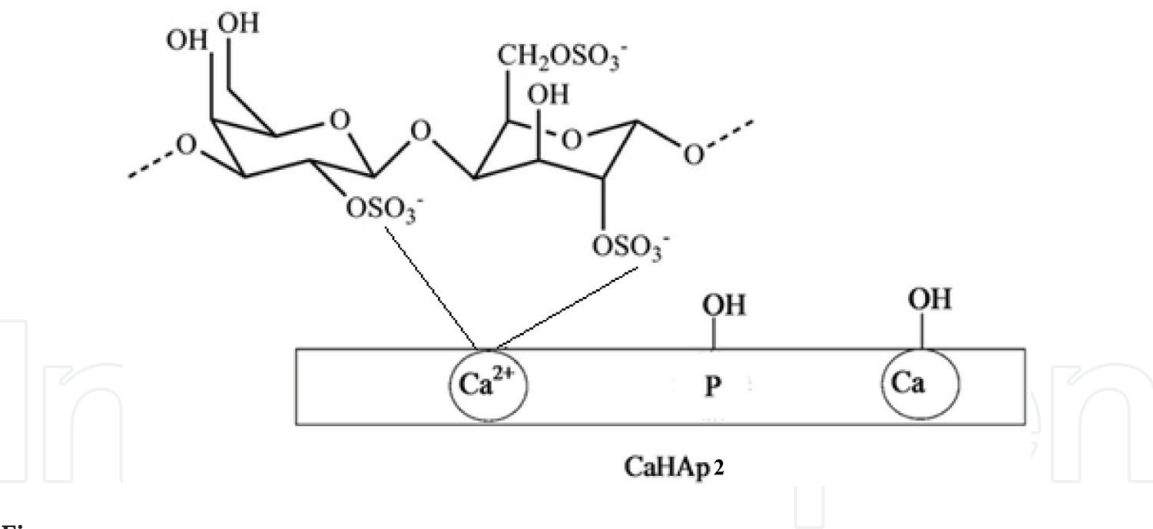


**Figure 7.**  
*Proposed mechanism of the interaction between (λ-Carr) and CaHAp2 surface.*

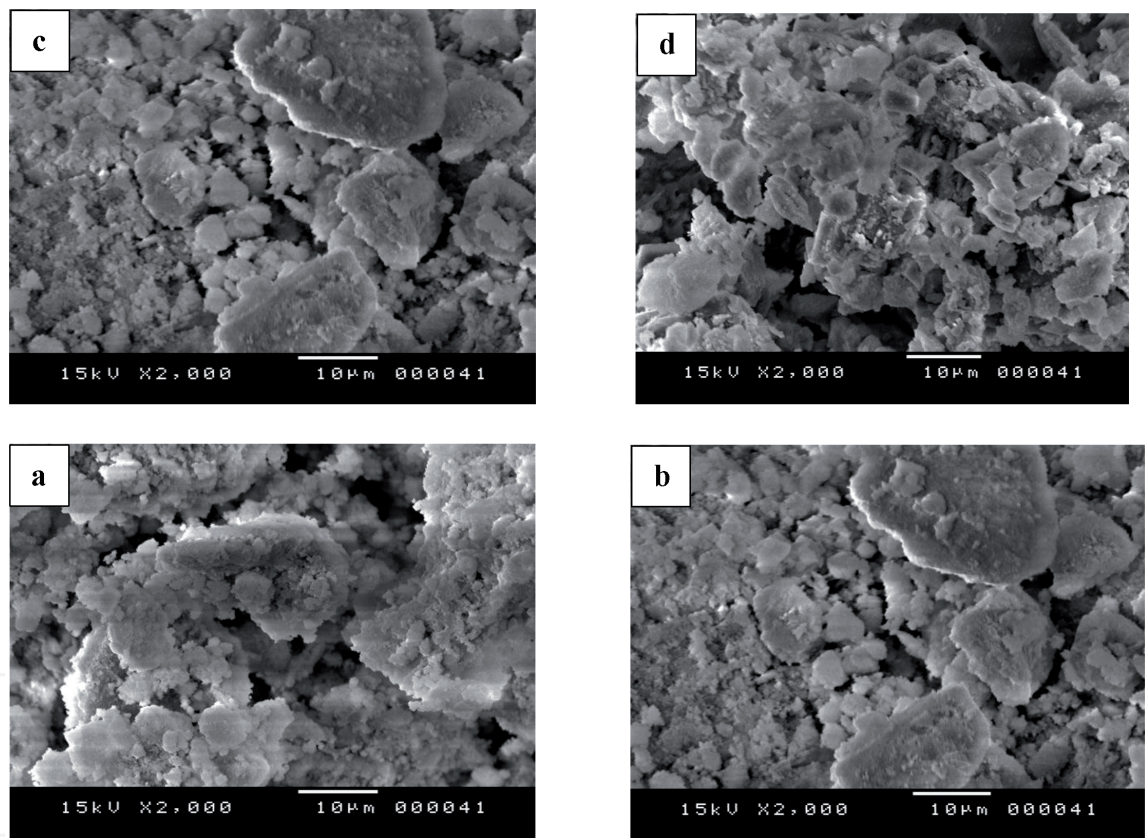


**Figure 8.**  
*SEM photomicrograph of modified hydroxyapatites: (a) CaHAp1, (b) CaHAp2, (c) CaHAp1-(Alg)10 and (d) CaHAp2-(Carr)10.*

of different sizes and poorly defined shape (**Figure 8(c, d)**). This change is due to the formation of new hybrid compounds CaHAp2-(λ-Carr) and CaHAp1-(Alg).

#### 4.1.4 Textural properties

The surface characteristics of the Hydroxyapatite samples obtained by the BET method, both before and after modification, are shown in **Table 1**. The treatment of hydroxyapatite with Alg biopolymer leads to the decreasing of specific surface area compared to that of ungrafted CaHAp1, covering the range from 20.52 to 3.39 m<sup>2</sup>/g. According to BET results, The fact that the surface area of CaHAp1-(Alg)5 and



Samples	Surface area (m <sup>2</sup> /g)
CaHAp1	21.64
CaHAp2	93.00
CaHAp1-(Alg)5	12.84
CaHAp1-(Alg)10	3.39
CaHAp2-(λ-Carr)5	168.00
CaHAp2-(λ-Carr)10	253.00
CaHAp2-(λ-Carr)20	260.00

**Table 1.**  
*Measurement of surface area of grafted hydroxyapatites.*

CaHAp1-(Alg)10 materials is lower than those in CaHAp1 can be explained with the filling of pores on the surface of hydroxyapatite by sodium alginate biopolymer. On the other hand, the specific surface of modified hydroxyapatite by lambda carrageenan increases with the increasing of grafting rate. The maximum value is obtained for CaHAp2-(λ-Carr) 20 (SSA = 260 m<sup>2</sup>/g).

**4.2 Evaluation of the performance of the prepared compounds for the adsorption of MB**

*4.2.1 Effect of pH*

**Figures 9 and 10** represent the variation of the adsorption capacity of MB on the surface of CaHAp1, CaHAp2, CaHAp1-(Alg) and CaHAp2-(λ-Carr) at different pH values. According to these figures, the MB removal increases gradually up to a pH very close to 5, and after kept nearly constant with further pH increase. The effect

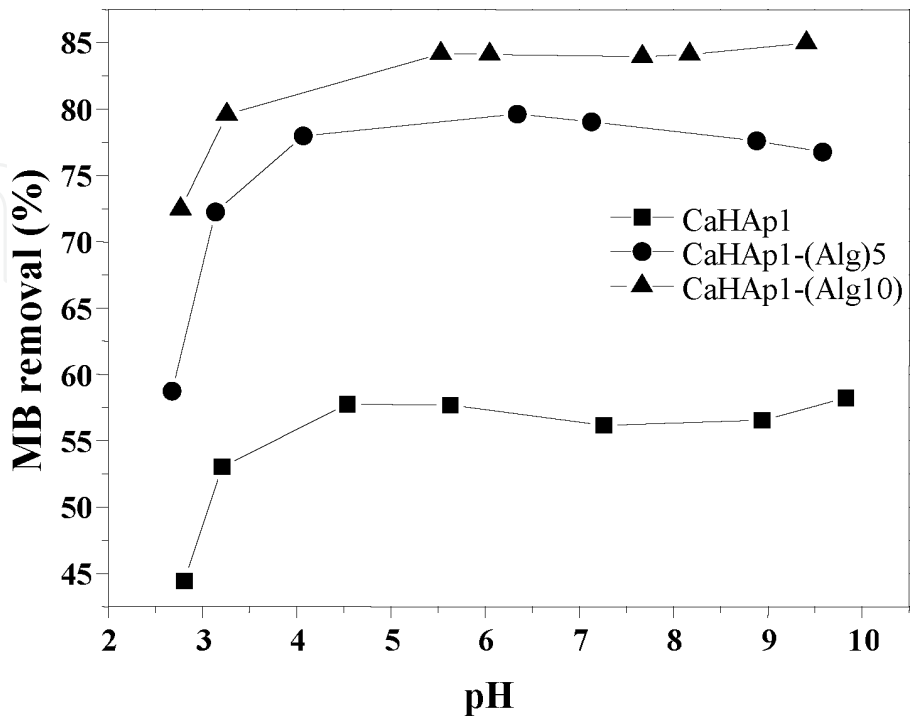


**Figure 9.**  
*Effect of initial pH on the adsorption of MB (Adsorbent dosage = 1 g/L, initial MB concentration = 50 mg/L, solution volume = 50 mL, temperature = 25°C, contact time = 3h).*

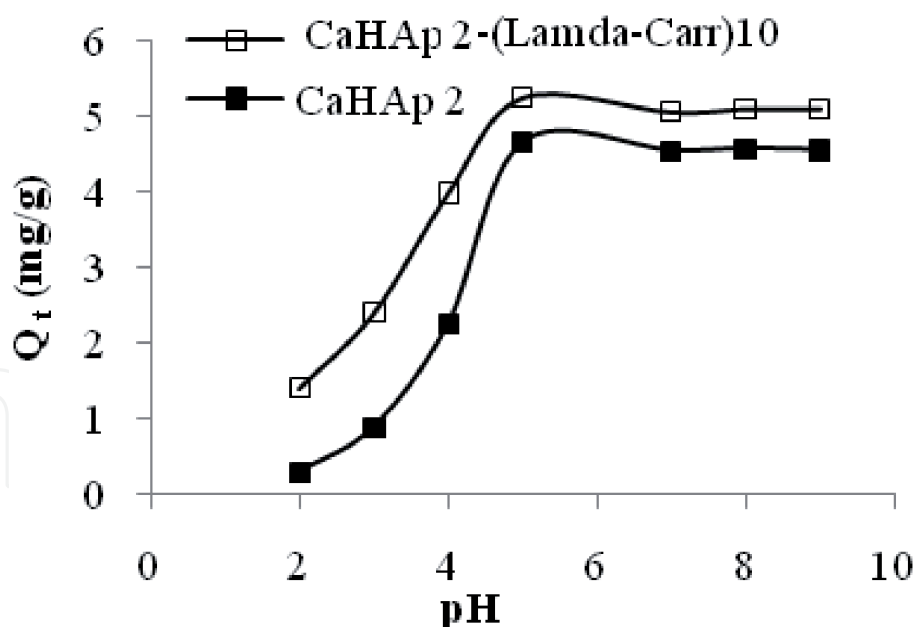


**Figure 10.**  
Effect of initial pH on the adsorption of MB (Adsorbent dosage = 1 g/L, initial MB concentration = 10 mg/L, solution volume = 25 mL, temperature = 25°C, contact time = 3 h).

of pH on adsorption depends on the point zero charge (pH pzc) of adsorbent. The value of pH<sub>pzc</sub> was found to be 6.2, 6.7 and 7.3 by CaHAp1, CaHAp2-(Carr)10 and CaHAp1-(Alg)10, respectively, in good agreement with literature data [31]. Indeed, for pH < pH<sub>pzc</sub>, the surface of hydroxyapatite is positively charged which causes the repulsion of cationic groups of the MB molecule ( $=N^+$ ), and hence low adsorption of dye. In the case of modified hydroxyapatite, the amount of dye adsorbed is higher than unmodified because (Alg) or ( $\lambda$ -Carr) contains carboxylate ( $-COO^-$ ) and sulphonate ( $OSO_3^-$ ) groups, respectively, that increase the interaction with dye molecules.

#### 4.2.2 Effect of contact time and adsorbent dose

The adsorptions of MB onto modified hydroxyapatites were studied with different biopolymer doses and at different periods of time. As shown in **Figures 11** and **12**, the adsorption amounts of MB on the modified hydroxyapatites increased rapidly with an increase in time and then became slower until the equilibrium was reached. Equilibrium is reached for all compounds prepared at low durations between 20 and 30 min. This may be due to the rapid saturation of the pores of our prepared adsorbents. The maximum adsorption is obtained for hydroxyapatite synthesized in the presence of biopolymer with 10% content. Therefore, the increase of MB removal with the increasing of adsorbent dose is mainly due to the increasing of interaction forces between the carboxylate groups ( $COO^-$ ) of (Alg) or sulphonate groups ( $OSO_3^-$ ) of ( $\lambda$ -Carr) and MB molecules via  $N^+$  groups. The possible modes of interaction between MB and either CaHAp1-(Alg) or or CaHAp2-( $\lambda$ -Carr) surface are given in **Figures 13** and **14**.

#### 4.2.3 Effect of temperature and initial dye concentration on the adsorption process

**Figures 15** and **16** shows the effect of temperature on the adsorption of MB on the surface of the prepared supports CaHAp1, CaHAp2, CaHAp1-(Alg) and CaHAp2-( $\lambda$ -Carr). As it is observed, the removal of MB by CaHAp2 increases with increasing the temperature of the solution from 25 to 60°C, indicating that

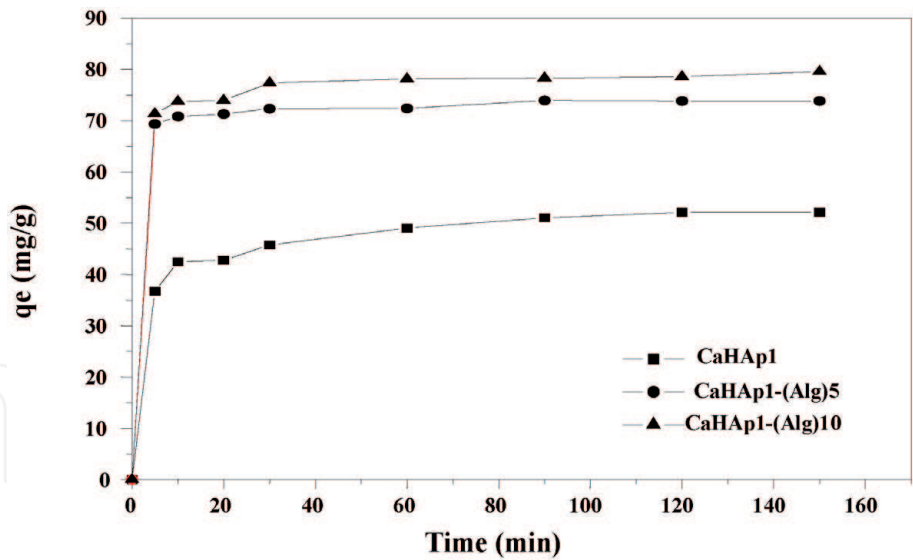


**Figure 11.** Effect of contact time on MB adsorption by CaHAp1 and CaHAp1-Alg (adsorption conditions: 0.05 g of adsorbent, initial MB concentration = 50 mg/L, solution volume = 50 mL,  $6 < \text{pH} < 7$ ,  $\text{rpm} = 110 \text{ tr/min}$  and temperature = 25 °C).

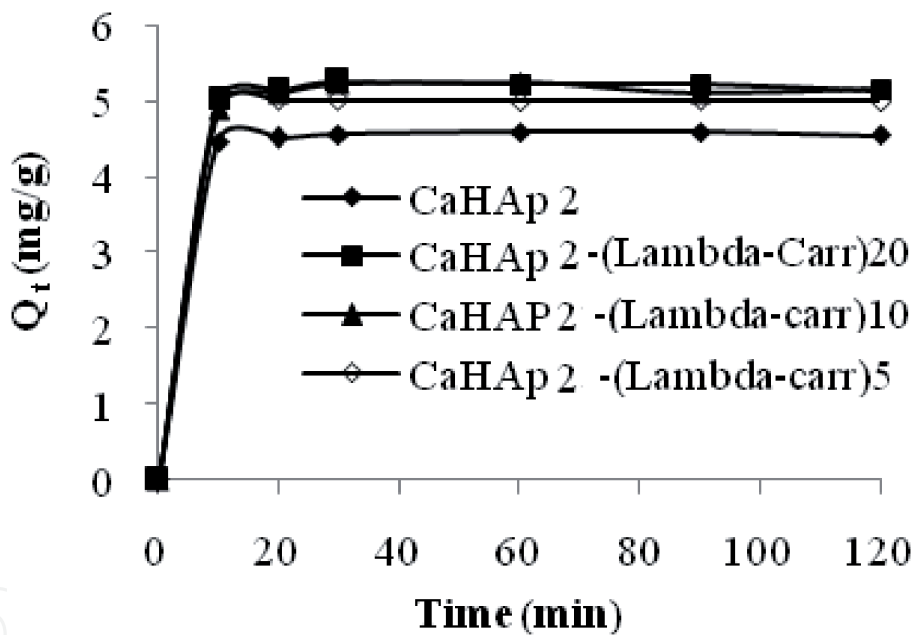


**Figure 12.** Effect of contact time on MB adsorption by CaHAp1 and CaHAp2-(λ-Carr) (adsorption conditions: 0.05 g of adsorbent, initial MB concentration = 50 mg/L, solution volume = 50 mL,  $6 < \text{pH} < 7$ ,  $\text{rpm} = 110 \text{ tr/min}$  and temperature = 25 °C).

the process is endothermic. In the case for other absorbents, the decrease of the adsorption of MB with the increase of temperature indicates that the adsorption is exothermic in nature.

This phenomenon could be explained by the decrease of the interaction between the MB ions and active sites in hydroxyapatite surface and the weakening of adsorptive forces between the carboxylate ( $\text{COO}^-$ ) groups of (Alg) or sulphate ( $\text{OSO}_3^-$ ) groups of ( $\lambda$ -Carr) and cationic dye molecules. As also depicted from **Figures 15 and 16**, the adsorbed amounts increase with the initial dye concentration to a threshold concentration corresponding to the saturation of the adsorption sites.

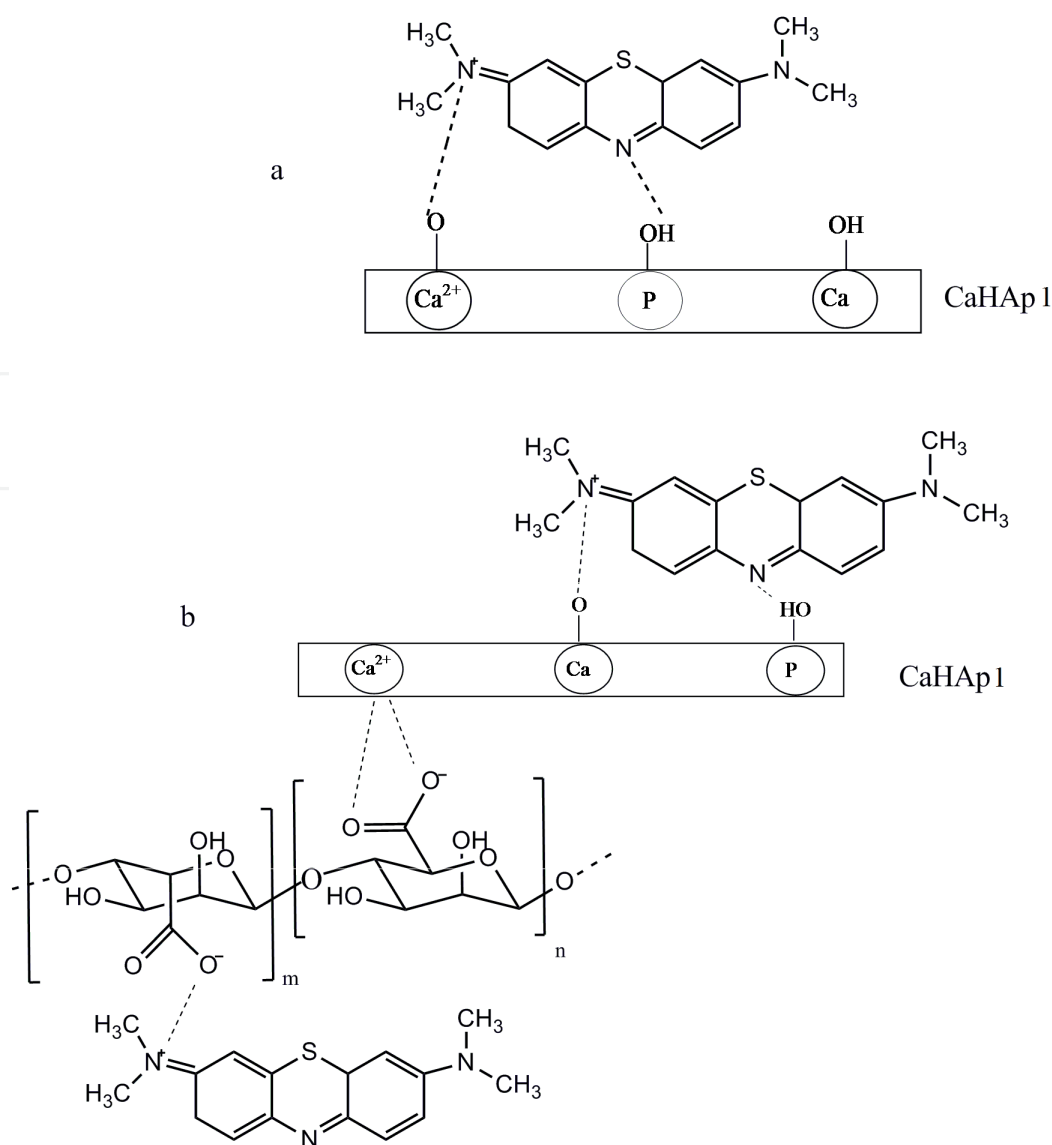


**Figure 13.**  
The possible modes of interaction between MB and either (a) CaHAp1 or (b) CaHAp1-(Alg).

According to these figures, the maximum adsorption capacity of CaHAp1-(ALg)10 is more important than those of CaHAp2-( $\lambda$ -Carr)10, CaHAp1 and CaHAp2. The adsorbed quantities are respectively 128.4, 98.23, 68.5 and 58.8 mg/g. Compared to other adsorbents gathered from the literature (**Table 2**), this registered amount of dye removal is so very interesting and thus our developed product could be seen as a good adsorbent.

In fact, this value is more important compared to garlic peel used as adsorbent (82.64 mg/g), Raw date pits (80.3 mg/g) and wood (84 mg/g). It is nearly twice higher compared to Wood ash (50 mg/g). It is five times more important than the Cotton waste (24 mg/g) and. It is six times important than modified pumice stone (15.87 mg/g) and Pure kaolin (15.55 mg/g). It is hundred times important than Fly ash (1.3 mg/g). Consequently, the above results confirmed that CaHAp-(Alg)10 was a favorable adsorbent for MB dye removal.

#### 4.2.4 Modeling and determination of kinetic parameters

In order to evaluate the kinetics involved in the process of the adsorption of MB dye onto CaHAp1, CaHAp2, CaHAp2-(Carr)10 and CaHAp1-(Alg)10 surface,

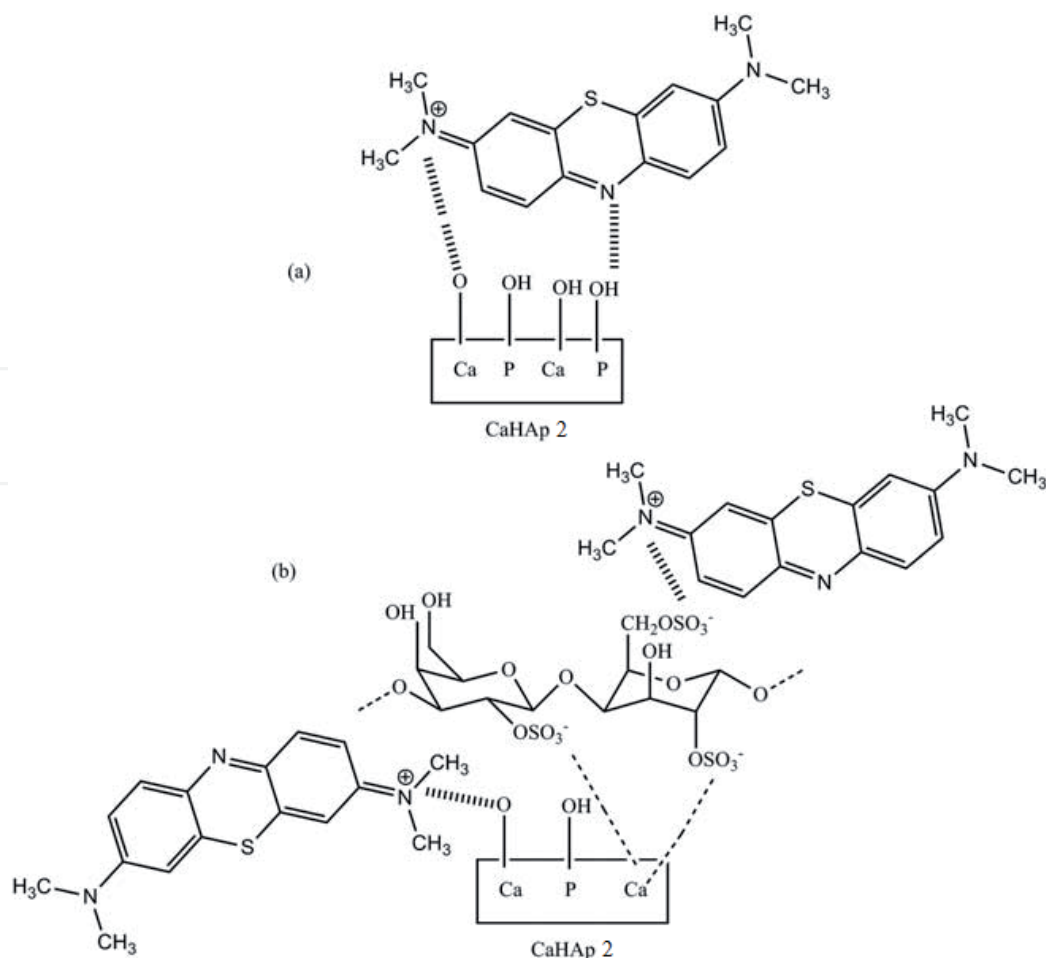


Figure 14.

The possible modes of interaction between MB and either (a) CaHAp2 or (b) CaHAp2-( $\lambda$ -Carr).

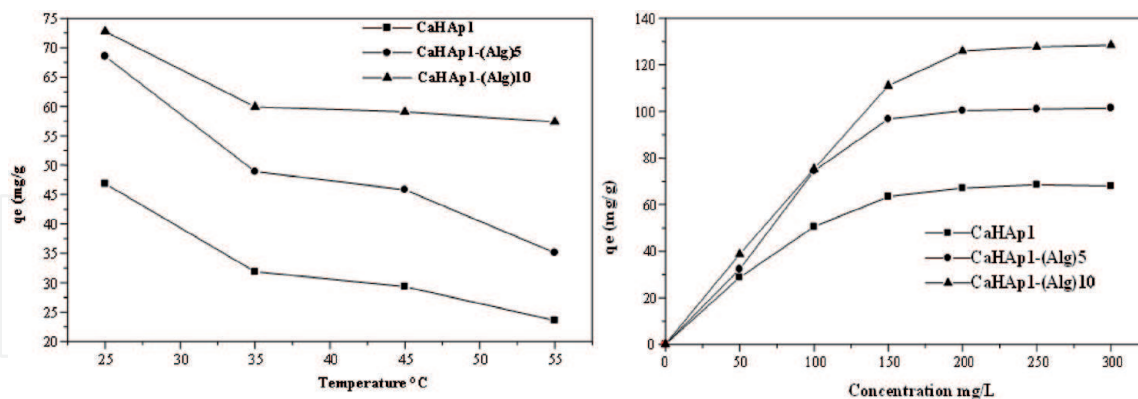


Figure 15.

Effect of temperature (a) and initial concentration (b) on the removal of MB using CaHAp1 and CaHAp1-(Alg).

pseudo-first-order, pseudo-second-order, Elovich, and intra-particle diffusion models were applied and results were discussed [42].

The results of the kinetic study, for hydroxyapatite synthesized in the presence of different amounts of Alg or ( $\lambda$ -Carr) are summarized in **Tables 3** and **4**. The best fit model was selected based on the linear regression correlation coefficient,  $R^2$  values. According to the regression coefficients ( $R^2 > 0.99$ ), the pseudo-second-order equation appears more suitable to describe the retention of MB on all prepared supports.



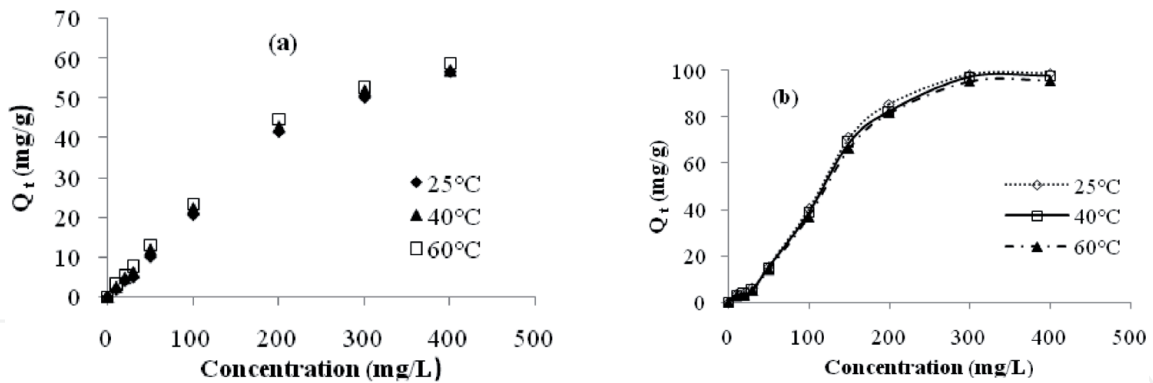


**Figure 16.**  
Effect of temperature on the removal of MB using: (a) CaHAp2 and (b) CaHAp2-(λ-Carr)10.

Samples	q <sub>m</sub> (mg/g)	References
CaHAp1-(Alg)10	128.40	In this work
Garlic peel	82.64	[32]
Wood ashes	50	[33]
Cotton waste	24	[34]
Modified pumice stone	15.87	[35]
Natural phosphate	7.23	[36]
natural zeolite	16.370	[37]
Raw date pits	80.30	[38]
Pure kaolin	15.55	[39]
Fly ash	1.3	[40]
Wood	84	[41]

**Table 2.**  
Comparison of the maximum BM adsorption capacity of the adsorbents in this study with other adsorbents.

Consequently, it can be confirmed that the adsorption is chemical and assumes that the surface of our adsorbent is heterogeneous.

4.2.5 Adsorption isotherm

In this study, Langmuir, Freundlich, Tempkin and Dubinin–Radushkevich (D-R) isotherm models were used to describe the adsorption of MB onto ungrafted and grafted hydroxyapatites [43].

The obtained parameters of each model are given in **Tables 5** and **6**. According to the analysis of regression coefficients ( $R^2$ ), Langmuir model has the highest value than those of the other models for modified hydroxyapatite by sodium alginate. This indicates that the Langmuir model appears appropriate for modeling the adsorption isotherms of MB on CaHAp1 or CaHAp1-(Alg) surface. As seen in **Table 5**, the  $R_L$  values [44] are situated within the range of  $0 < RL < 1$ , which means that prepared CaHAp or CaHAp-(Alg) is favorable for the adsorption of MB dye under the experimental conditions conducted in this study.

For modified hydroxyapatite by lambda carrageenan, the analysis of regression coefficients shows better applicability of Freundlich model. Moreover, in all compounds, the values of calculated  $n$  are less than 1, indicating that the adsorption of MB is favorable.

	Pseudo-first-order			Pseudo-second-order			Elovich		Intra-particle diffusion		
	$K_1$	$q_e$	$R^2$	$K_2$	$q_e$	$R^2$	$\alpha$	$\beta$	$R^2$	$K_i$	$R^2$
0%	0.0234	16.764	0.8305	0.00648	52.910	0.9991	12.946	12.210	0.8131	3.0578	0.6086
5%	0.149	4.769	0.3244	0.02641	74.074	0.9999	28.701	11.128	0.5838	3.505	0.3675
10%	0.0181	7.197	0.4388	0.01556	79.365	0.9999	28.931	8.903	0.6240	3.9032	0.4046

**Table 3.**  
*Kinetic constants for the adsorption of studied dyes on hydroxyapatite-Alginate ( $T = 25^{\circ}\text{C}$ ,  $C_o = 100 \text{ mg/L}$ ,  $6 < \text{pH} < 7$ ).*

	Pseudo-first-order			Pseudo-second-order			Elovich			Intra-particle diffusion	
	K <sub>1</sub>	q <sub>e</sub>	R <sup>2</sup>	K <sub>2</sub>	q <sub>e</sub>	R <sup>2</sup>	α	β	R <sup>2</sup>	K <sub>i</sub>	R <sup>2</sup>
0%	0.0088	0.41	0.346	2.7	4.58	0.999	7.49 <sup>E18</sup>	10.41	0.670	0.317	0.488
5%	0.0085	0.29	0.271	5.51	5.02	1	1.33 <sup>E57</sup>	27.24	0.457	0.344	0.476
10%	0.0075	0.53	0.247	-20.86	5.162	0.999	1.31 <sup>E10</sup>	5.17	0.378	0.361	0.498
20%	0.0079	0.34	0.2	-1.18	5.184	0.999	3.67 <sup>E15</sup>	7.62	0.349	0.361	0.489

**Table 4.**  
Kinetic constants for the adsorption of studied dyes on hydroxyapatite-Carrageenan (*T* = 25°C, *C*<sub>0</sub> = 10 mg/L, *pH* = 5).

Isotherm model	Adsorption constant	Adsorbent		
		CaHAp1	CaHAp1-(Alg)5	CaHAp1-(Alg)10
Langmuir	q max (mg/g)	77.51	117.64	142.85
	K <sub>L</sub> (l/mg)	0.038	0.041	0.062
	R <sub>L</sub>	0.34-0.08	0.33-0.07	0.25-0.04
	R <sup>2</sup>	0.994	0.974	0.992
Freundlich	n	2.876	0.468	0.541
	K <sub>F</sub> (l/mg)	11.762	0.0028	0.0209
	R <sup>2</sup>	0.864	0.827	0.685
Temppkin	B <sub>1</sub>	18.462	0.032	0.028
	K <sub>T</sub>	0.286	3.8 · 10 <sup>19</sup>	4.6 · 10 <sup>13</sup>
	R <sup>2</sup>	0.946	0.777	0.886
D-R	q max (mg/g)	66.62	105.50	120.50
	K <sub>D-R</sub> (mol <sup>2</sup> /J <sup>2</sup> )	6·10 <sup>-5</sup>	5·10 <sup>-5</sup>	2·10 <sup>-5</sup>
	E (KJ/mol)	91.28	100	158.11
	R <sup>2</sup>	0.97	0.95	0.94

**Table 5.**  
Isotherm constants and correlation coefficients (*R*<sup>2</sup>) for MB adsorption on the surface of CaHAp1 and CaHAp1-(Alg) at different temperatures.

The values of *E* calculated from Dubinin-Redushkevich equation are greater than 40 KJ mol<sup>-1</sup> for all samples, which confirms that the adsorption is chemical [42].

4.2.6 Determination of the thermodynamic parameters

The standard Gibbs free energy change ( $\Delta G^\circ$ ) has been determined from the following equation [21].

$$\Delta G^\circ = -RT \ln K_L \tag{4}$$

Where *R* is the universal gas constant (8.314 J mol<sup>-1</sup> K<sup>-1</sup>), *T* is the temperature (K) and *K<sub>L</sub>* value is the Langmuir equilibrium constant. The enthalpy change  $\Delta H^\circ$

Langmuir constants				Freundlich constants			Temkin constants			Dubinin-redushkevich constants			Thermodynamic parameters		
CaHAp2															
T (°C)	K <sub>L</sub>	q <sub>m,L</sub>	R <sup>2</sup>	K <sub>F</sub>	n <sub>F</sub>	R <sup>2</sup>	B <sub>T</sub>	A <sub>T</sub>	R <sup>2</sup>	Q <sub>m,DR</sub>	E	R <sup>2</sup>	ΔH°	ΔS°	ΔG°
25	0.017	285.7	0.407	0.51	1.03	0.990	36.85	0.29	0.916	3.84	70.71	0.596	42.3	0.25	−32.2
40	0.025	156.2	0.851	0.62	1.12	0.991	37.1	0.30	0.925	3.98	70.71	0.588			−26.95
60	0.026	125	0.944	0.73	1.21	0.993	37.52	0.31	0.928	4.1	79.05	0.572			−40.95
CaHAp2-(λ-Carr)10															
25	0.005	588.2	0.161	0.894	0.951	71.75	0.289	0.909	4.9	70.71	0.483	0.328	−3.1	−29.2	8.69
40	0.005	526.3	0.189	0.89	0.953	70.52	0.288	0.909	4.85	70.71	0.481	0.323			9.13
60	0.004	500	0.181	0.87	0.955	69.32	0.286	0.905	4.77	70.71	0.486	0.314			9.7

**Table 6.**  
*Isotherm constants and thermodynamic parameters for dye adsorption on the surface of CaHAp2 and CaHAp2-(Carr)10 at different temperatures.*

	$\Delta H^\circ$ (KJ/mol)	$\Delta S^\circ$ (KJ/mol)	$\Delta G^\circ$ (KJ/mol)			
			298°K	308°K	318°K	328°K
CaHAp1	-27.96	-0.094	0.218	1.163	2.109	3.055
CaHAp1-Alg(10)	-20.432	-0.059	-2.789	-2.197	-1.605	-1.013

**Table 7.**  
*Values of thermodynamic parameters for MB dye removal with CaHAp1 and CaHAp1-Alg.*

and entropy change  $\Delta S^\circ$  of the adsorption were estimated from the following equation:

$$\text{Ln}K_L = -\frac{\Delta H^\circ}{RT} + \frac{\Delta S^\circ}{R} \tag{5}$$

The values of  $\Delta H^\circ$  and  $\Delta S^\circ$  were determined from the slopes and intercept of the linear plot of  $\text{Ln} K_L$  versus  $(1/T)$ . The calculated thermodynamic parameters are summarized in **Tables 6** and **7**.

The values of the enthalpy  $\Delta H^\circ$  indicates that the adsorption process is endothermic for CaHAp2 ( $\Delta H^\circ > 0$ ), and exothermic for (CaHAp1, CaHAp2-( $\lambda$ -Carr)10, CaHAp1-(Alg)10) ( $\Delta H^\circ < 0$ ). The  $\Delta G^\circ$  values were negative for (CaHAp2, CaHAp1-(Alg)10) and positive for (CaHAp1, CaHAp2-( $\lambda$ -Carr)10).

The positive  $\Delta G^\circ$  values indicates that the instability activation complex of the adsorption reaction increases with increasing temperature, The negative values of  $\Delta G^\circ$  means that the process is feasible and adsorption is spontaneous thermodynamically [45].

The negative value of entropy  $\Delta S^\circ$  confirms the decreased randomness at the solid–solution interface during adsorption.

**5. Conclusion**

In this study, the results of characterization techniques IR, XRD, SSA and SEM analysis showed that the sodium alginate or lambda carrageenan were successfully grafted on the hydroxyapatite surface. The modified hydroxyapatite could be potentially applied for the removal of methylene blue dye from aqueous solution. The determination of the amount of dye adsorbed on the various apatitic phase CaHAp1, CaHAp2, CaHAp1-(Alg) and CaHAp2-( $\lambda$ -Carr) allowed us to build the adsorption isotherms which give information on the adsorption mechanism. The Modeling of the isotherms proved that the adsorption of MB on modified hydroxyapatite is described by the Freundlich equation for CaHAp2-( $\lambda$ -Carr) and Langmuir for CaHAp1-(Alg). The calculated adsorption capacities of CaHAp1, CaHAp2, CaHAp1-Alg10 and CaHAp2-( $\lambda$ -Carr)10 for MB, at 25°C, were 68.5, 58.8 128.40, and 98.23 mg/g, respectively. The results gave a clear indication that the modified hydroxyapatite has a great capacity than pure hydroxyapatite for dye removal.

Thermodynamic studies indicated that the physic-sorption is the dominating mechanism for the dye adsorption process onto CaHAp1-(Alg)10 or CaHAp2-( $\lambda$ -Carr)10, spontaneous and exothermic in nature. The results indicate that the modified hydroxyapatite CaHAp2-( $\lambda$  Carr) or CaHAp1-(Alg) possessed good adsorption ability towards MB dye and can be used as a low cost adsorbent for other



environmental applications as retention of heavy metal and pesticides from wastewater. Further works will be extended for the functionalization of hydroxyapatite materials with surfactants and cationic reagents for the removal of organic pollutants from contaminated waters.

## Acknowledgements

The authors thank the INRAP (Institut Nationale de Recherche et d'Analyses Physico-chimiques), INRST (Institut Nationale de Recherche Scientifique et Technologique), ETAP (Entreprise Tunisienne d'Activités Pétrolières) and the University of El Manar and Monastir (Tunisia).

## Author details

Hassen Agougui<sup>1,2\*</sup>, Youssef Guesmi<sup>3,4</sup> and Mahjoub Jabli<sup>5,6</sup>

1 Faculty of Sciences of Gafsa, University of Gafsa, University Campus, Zarroug, Gafsa, Tunisia

2 Laboratory of Physical-Chemistry of Materials, Faculty of Sciences of Monastir, Monastir, Tunisia

3 Laboratory, Water, Membrane and Environmental Biotechnology, Centre of Research and Water Technologies, Technopark of Borj-Cedria, Soliman, Tunisia


4 Faculty of Sciences of Tunis, University of Tunis - El Manar, Tunis, Tunisia

5 Department of Chemistry, College of Science Al-zulfi, Majmaah University, Al-Majmaah, Saudi Arabia

6 Textile Materials and Processes Research Unit, Tunisia National Engineering School of Monastir, University of Monastir, Tunisia

\*Address all correspondence to: [hassenagougui@yahoo.fr](mailto:hassenagougui@yahoo.fr)

## IntechOpen

© 2021 The Author(s). Licensee IntechOpen. This chapter is distributed under the terms of the Creative Commons Attribution License (<http://creativecommons.org/licenses/by/3.0>), which permits unrestricted use, distribution, and reproduction in any medium, provided the original work is properly cited. 

## References

- [1] D. Suteu, S. Coseri, C. Zaharia, G. Biliuta, I. Nebunu, *Desalination Water Treat.* 90 (2017) 341-349
- [2] G. Annadurai, R.S. Juang, D.J. Lee, J. Hazard. Mater. 92 (2002) 263-274
- [3] S. A. Shahid Chatha, M. Asgher, S. Ali, A. Ijaz Hussain, *Carbohydr. Polym.* 87 (2012) 1476-1481.
- [4] M. R. Fat'hi, A. Ahmadi, *Int J Env Health Eng.* (2016) 5-19
- [5] S. Masoudnia, M. H. Juybari, R. Zafar Mehrabian, M. Ebadi, F. Kaveh, *Int. J. Biol. Macromol.* 165 (2020) 118-130.
- [6] G. J. Copello, A. M. Mebert, M. Raineri, M. P. Pesenti, L. E. Diaza, *J. Hazard. Mater.* 186 (2011) 932-939.
- [7] Y. Wang, Y. Peib, W. Xiong, T. Liud, J. Li, S. Liu, B. Li, *Int. J. Biol. Macromol.* 81 (2015) 477-482.
- [8] N. A. Zakharov, Zh. A. Ezhova, E. M. Koval, V. T. Kalinnikov, and A. E. Chalykh, *Inorg. Mater.* 41 (2005) 509-515.
- [9] R. Khanna, K. S. Katti, and D. R. Katti, *J. Polym. Sci.* 2010 (2010) 1-12.
- [10] D. Wahl and J. Czernuszka, *Eur Cell Mater.* 11 (2006) 43-56.
- [11] K. Senthilarasan, A. Ragu and P. Sakthivel, *Int. J. Eng. Res. Appl.* 4 (2014) 55-59.
- [12] N. Koupaei, A. Karkhaneh, J. Tissue. *Eng. Regen. Med.* 13 (2016) 251-260.
- [13] K. Kanimozhi, D. Gopi and L. Kavitha, *Int. J. Eng. Sci. Eng. Res.* 5 (2014) 138-140.
- [14] H. Hou, R. Zhou, P. Wu, L. Wu, *Chem. Eng. J.* 211-212 (2012) 336-342.
- [15] M. C. Chang, C. Chang Ko, W. H. Douglas, *Biomaterials.* 24 (2003) 2853-2862.
- [16] M. Vila, S. Sánchez-Salcedo, M. Cicuéndez, I. Izquierdo-Barba, María Vallet-Regí, *J. Hazard. Mater.* 192 (2011) 71-77.
- [17] K. Sangeetha, G. Vasugi, E. K. Girija, *Int. J. Chem. Tech. Res.* 8 (2015) 117-125.
- [18] G. Vasugi and E. K. Girija, *Chem. Technol.* 49 (2015) 87-91.
- [19] W. Wei, R. Sun, Z. Jin, J. Cui, Z. Wei, *Appl. Surf. Sci.* 292 (2014) 1020-1029.
- [20] U. Nadeem and M. Datta, *Eur. Chem. Bull.* 3 (2014) 682-691.
- [21] H. Hou, R. Zhou, P. Wu, L. Wu, *Chem. Eng. J.* 211-212 (2012) 336-342.
- [22] A. K. Radzimska, M. Samuel, D. Paukszta, A. Piaseck, T. Jesionowsk, *Physicochem. Probl. Miner. Process.* 50 (2014) 225-236.
- [23] H. Eslami, M. S. Hashjin, M. Tahriri, *Iranian J. Pharm. Sci.* 4 (2008) 127-134.
- [24] K. Allam, A. El Bouari, B. Belhorma, L. Bih, *J.WA.R.P.* 8 (2016) 358-371.
- [25] A. Aissa, H. Agougui, M. Debbabi, *Appl. Surf. Sci.* 257 (2011) 9002-9007.
- [26] H. Agougui, A. Aissa, S. Maggi, M. Debbabi, *Appl. Surf. Sci.* 257 (2010) 1377.
- [27] M. Othmani, A. Aissa, H. Bachoua, M. Debbabi, *Appl. Surf. Sci.* 264 (2013) 886-891.
- [28] L. Sukhodub, *Mater. Sci. Technol.* 40 (2009) 318-325.

- [29] Malik, Z. M.; Jarmoluk, K. M. A. *Polymer*. 8 (2016) 275.
- [30] N.A. Kamalaldin, B.H. Yahya, A. Nurazreena, *Procedia. Chem.* 19 (2016) 297-303.
- [31] Wei, W.; Yang, L.; Zhong, W. H.; Li, S. Y.; Cui, J.; Wei, Z. G. *Dig. J. Nanomater. Biostruct.* 10 (2015) 1343.
- [32] B.H. Hameed, A.A. Ahmad, *J. Hazard. Mater.* 164 (2009) 870-875.
- [33] N. E. Fayoud, S. A. Younssi, S. Tahiri, A. A. Albizane, *J. Mater. Environ. Sci.* 6 (2015) 3295-3306.
- [34] G. McKAY, G. RAMPRASAD, P. PRATAPA MOWLI, *Water, Air, and Soil Pollution*. 29 (1986) 273-283.
- [35] Z. Derakhshan, M. A. Baghapour, M. Ranjbar, M. Faramarzian, *Health Scope*. 2 (2013) 136-144.
- [36] N. Barka, A. Assabbane, A. Nounah, L. Laanab, Y.A. Ichou, *Desalination*. 235 (2009) 264-275.
- [37] Runping Han,, Jingjing Zhang, Pan Han, Yuanfeng Wang, Zhenhui Zhao, Mingsheng Tang, *Chem. Eng. J.* 145 (2009) 496-504.
- [38] F. Banat, S. Al-Asheh, L. Al-Makhadmeh, *Process Biochem.* 39 (2003) 193-202.
- [39] D. Gosh, G. Bhattacharyya, *Appl. Clay. Sci.* 20 (2002) 295-300.
- [40] C. Woolard, J. Strong, C. Erasmus, *Appl Geochem.* 17 (2002) 1159-1164.
- [41] G. McKay, V. Poots, *J. Chem. Technol. Biotechnol.* 30 (1986) 279-282
- [42] Runping, H.; Pan, H.; Zhaohui, C.; Zhenhui, Z.; Mingsheng, T. *J. Environ. Sci.* 2008, 20, 1035.
- [43] W. Wei, L. Yang, W.H. Zhong, S.Y. Li, J. Cui, Z.G. Wei, *Dig. J. Nanomater. Biostruct.* 10 (2015) 1343-1363.
- [44] D. Robati, B. Mirza, R. Ghazisaeidi, M. Rajabi, O. Moradi, S. Agarwal, V.K. Gupta, I. Tyagi, *J. Mol. Liq.* 216 (2016) 830-835.
- [45] Z. Jia, Z. Li, S. Li, Y. Li, R. Zhu, *J. Mol. Liq.* 220 (2016) 56-62.